Polymer Chemistry

PAPER

Polymerization-induced self-assembly: ethanolic RAFT dispersion polymerization of 2-phenylethyl methacrylate

Cite this: DOI: 10.1039/c3py01719b

Yiwen Pei and Andrew B. Lowe*

Received 16th December 2013
Accepted 6th January 2014

DOI: 10.1039/c3py01719b

www.rsc.org/polymers

Reversible addition-fragmentation chain transfer (RAFT) radical dispersion polymerization (RAFTDP) has been employed to polymerize 2-phenylethyl methacrylate (PEMA) using poly[2-(dimethylamino)ethyl methacrylate] (PDMAEMA) macromolecular chain transfer agents (macro-CTAs) of varying average degree of polymerization ($\bar{X}_n$). RAFTDP of PEMA in ethanol at 70 °C with PDMAEMA macro-CTAs yields well-defined AB diblock copolymers that self-assemble in solution during polymerization leading to the formation of well-defined diblock copolymer nanostructures. A full morphology transition (from spheres to worms to vesicles) is observed with these formulations that is sensitive to (i) the target $\bar{X}_n$ of the solvophobic polyPEMA block, (ii) the total solids content at which the PEMA block copolymerization is performed and (iii) the target $\bar{X}_n$ of PDMAEMA as a macro-CTA. Finally, we demonstrate the ability to convert the PDMAEMA–PPEMA based nanoparticles to the corresponding sulfopropylbetaine analogues by the facile reaction of the DMAEMA residues with 1,3-propanesultone.

Introduction

Reversible-deactivation radical polymerizations, such as reversible addition-fragmentation chain transfer (RAFT) polymerization,[1–5] are well-established and highly efficient techniques for the synthesis of diblock copolymers with predetermined compositions, molecular weights and low dispersities ($Đ_M = \bar{M}_w/\bar{M}_n \leq 1.40$). Indeed, there is now extensive literature on the synthesis, properties, and applications of such materials.[6–10] Part of the interest in AB diblock copolymers stems from the fact that in a selective solvent, or solvent mixture, such species can self-assemble into a wide range of nano-to-micron sized species including spherical micelles,[11,12] rod-like micelles (also termed cylindrical micelles or worms),[13–15] vesicles (also known as polymersomes or niosomes)[12,16–18] and other complex intermediate and higher ordered aggregates. While such assembled species have been studied for many decades they are currently receiving significant attention in fields such as nanomedicine,[19–21] MRI imaging[22] and as templates[23] and nanoreactors.[24]

Historically, the preparation of such self-assembled polymeric particles has involved synthesis, isolation, and characterization of a parent AB diblock copolymer followed by often time consuming protocols to induce self-assembly in dilute solution in a selective solvent (a copolymer concentration $\leq$ 1.0 wt% is common).[25,26] Alternatively, an external trigger, such as a change in solution pH or temperature, can be employed in diblock copolymers that contain an appropriate stimulus-responsive block, *i.e.* one that changes from being solvophilic to solvophobic upon application of the applied stimulus, to induce self-assembly.[27]

Recently, there has being growing interest in polymerization systems that allow for *simultaneous* block copolymer formation and self-assembly in solution, an approach termed polymerization-induced self-assembly (PISA). In particular, RAFT dispersion polymerization (RAFTDP) has recently been attracting significant attention.[28,29] This is due to the fact that RAFTDP has the advantages of a conventional bulk or homogeneous solution RAFT polymerization coupled with the desirable benefits of a heterogeneous process including the ability to prepare particles at high solids content, low solution viscosities and improved polymerization kinetics.

Compared to homogeneous RAFT polymerization there is relatively little in the literature regarding RAFTDP. One of the earliest reports came from An *et al.*[30] who reported the RAFTDP of *N*-isopropylacrylamide (NIPAM) employing poly(*N*,*N*-dimethylacrylamide) (PDMA) macro chain transfer agents (macro-CTAs) in water at 70 °C. At this temperature, *i.e.* above the lower critical solution temperature of polyNIPAM, the resulting block copolymer existed in a self-assembled state that could be locked *via* the addition of a difunctional crosslinker. Cooling the solution without adding crosslinker resulted in molecular dissolution since both blocks are hydrophilic at ambient temperature. Since this early contribution several groups have evaluated RAFTDP for its versatility in the direct preparation of nanosized particles. Armes *et al.* have conducted a series of

Centre for Advanced Macromolecular Design (CAMD), School of Chemical Engineering, The University of New South Wales, Kensington, Sydney, NSW 2052, Australia. E-mail: a.lowe@unsw.edu.au; Tel: +61 2 9385 6031

studies on all-polymethacrylic systems in both aqueous[31–37] and alcoholic[38–40] media. For example, Zehm, Ratcliffe and Armes[40] detailed the alcoholic RAFTDP of benzyl methacrylate (BzMA) with poly(2-hydroxyethyl methacrylate) (PHEMA) or poly(2-hydroxypropyl methacrylate) (PHPMA) macro-CTAs. A benefit of such all-methacrylic systems is the ability to prepare a variety of morphologically distinct nanoparticles while simultaneously achieving near-quantitative monomer conversions. A detailed evaluation of the effect of alcoholic solvent, total solids content, average degree of polymerization ($\bar{X}_n$) of the BzMA block and the $\bar{X}_n$ of the stabilizing blocks was reported. Charleux and co-workers have described several different systems including poly(ethylene oxide-*block*-dialkylacrylamide)s in aqueous media,[41] and poly(2-ethylhexyl acrylate-*block*-methyl methacrylate-*block*-2-ethylhexyl acrylate) ABA triblocks prepared in isododecane with a poly(2-ethylhexyl acrylate) macro CTA which gave particles with sizes ranging from 100 to 300 nm.[42] Pan *et al.* have also studied a variety of methanolic RAFTDP PISA systems including those yielding poly(acrylic acid-*block*-styrene) assemblies,[43] poly(4-vinylpyridine-*block*-styrene) aggregates,[44,45] and poly(ethylene oxide-*block*-styrene) copolymers which are capable of forming nano-objects with a variety of morphologies including spheres, wires and vesicles.[46] Finally, we note it is also possible to conduct RAFTDP in non-conventional solvents such as supercritical CO_2 ($scCO_2$) as exemplified by the work of Howdle *et al.*[47,48]

Even though the body of literature dealing with RAFTDP and PISA is growing there is still a relatively limited number of monomers that have been employed as the core-forming blocks – styrene, several commonly employed methacrylates and examples of thermoresponsive acrylamido species. Inspired by the above reports we have recently initiated a program aimed at evaluating new, less common, monomers as potential insoluble blocks in RAFTDP formulations. Herein, we report the one-pot, ethanolic RAFTDP of 2-phenylethyl methacrylate (PEMA) employing poly[2-(dimethylamino)ethyl methacrylate]s as macro-CTAs. To the best of our knowledge the RAFTDP of PEMA has never before been reported, but is an interesting building block given the documented high refractive index of its homopolymer and its use as a foldable intraocular lens material.[49] A systematic study for this formulation is constructed by varying the target $\bar{X}_n$ of the solvophobic polyPEMA and solvophilic poly[2-(dimethylamino)ethyl methacrylate] blocks, as well as evaluating the total solids content of the polymerizations and determining their effect on the resulting particle morphology.

Experimental

Materials

All reagents were purchased from the Sigma-Aldrich Chemical Company and used as received unless otherwise noted. 2,2′-Azobis(isobutyronitrile) (AIBN) was purified by recrystallization twice from methanol. 2-(Dimethylamino)ethyl methacrylate (DMAEMA) and 2-phenylethyl methacrylate (PEMA) were passed through a basic Al_2O_3 column to remove the inhibitor prior to use. 4-Cyanopentanoic acid dithiobenzoate (CPADB) was prepared according to a procedure described elsewhere.[50]

Synthesis of poly[2-(dimethylamino)ethyl methacrylate] macro-CTA

A general procedure for the RAFT homopolymerization of DMAEMA mediated by CPADB is as follows.

A solution containing 2-(dimethylamino)ethyl methacrylate (DMAEMA) (10 g, 0.06 mol), CPADB (0.3 g, 1.06 mmol), AIBN (27 mg, 0.17 mmol) and acetonitrile (10 mL) was added to a reaction vessel equipped with a magnetic stir bar. The reaction vessel was sealed and the solution purged with nitrogen for 15 min prior to being placed in a preheated oil bath at 70 °C. The DMAEMA homopolymers(s) were isolated by precipitation into *n*-hexane followed by filtration and then dried at 40 °C under vacuum overnight.

Synthesis of poly[2-(dimethylamino)ethyl methacrylate-*block*-2-phenylethyl methacrylate] (PDMAEMA-*b*-PPEMA) copolymer particles *via* RAFT dispersion polymerization in ethanol

In a typical RAFT dispersion polymerization synthesis conducted at 29 wt% total solids, PEMA (0.5 g, 2.62 mmol), AIBN (0.86 mg, 0.005 mmol), $PDMAEMA_{45}$ macro-CTA (176 mg, 0.026 mmol), and triethylamine (10 mol% excess based on DMAEMA residues) were dissolved in ethanol (1.72 g). The reaction mixture was sealed in a reaction vessel, purged with nitrogen gas and then placed in a preheated oil bath at 70 °C for 18 h. The final monomer conversion was determined by ^{1}H NMR analysis by integrating the PPEMA peak (CH_3) at 2.32 ppm to PEMA monomer vinyl peak (CH_2) at 5.5 and 6.1 ppm.

Reaction of $PDMAEMA_{45}$-*b*-$PPEMA_{98}$ with 1,3-propanesultone

Betainization of the DMAEMA residues in the $PDMAEMA_{45}$-*b*-$PPEMA_{98}$ block copolymers was performed in ethanol using a 10 mol% excess of 1,3-propanesultone relative to DMAEMA repeat units. The reaction was carried out overnight at room temperature. At the end of the reaction, the betainized block copolymer ($PDMAEMASB_{45}$-*b*-$PPEMA_{98}$) was obtained as a white precipitate, which was isolated by filtration and then washed with ethanol to remove unreacted 1,3-propanesultone. The resulting betainized block copolymer was then dried under vacuum overnight at 40 °C. The extent of betainization was determined by ^{1}H NMR spectroscopy. The betaine block copolymer was directly re-dispersed in water *via* gentle stirring for TEM analysis.

Copolymer characterization

NMR spectroscopic measurements were performed on a Bruker DPX 300 instrument at 300 MHz for hydrogen nuclei. The internal solvent signal of $CDCl_3$ was used as reference (δ ($CHCl_3$) = 7.26 ppm). The number average molecular weight, $\bar{M}_{n,NMR}$, and the average degree of polymerization, $\bar{X}_n$, were estimated based on the integral values of the signals at δ = 4.06 ppm and 7.30–7.90 ppm, as shown in eqn (1).

$$\bar{X}_n(\text{PDMAEMA}) = 5 \times I\,(4.06\text{ ppm})/2 \times I\,(7.30\text{–}7.90\text{ ppm}) \quad (1)$$

where I (4.06 ppm) and I (7.30–7.90 ppm) are the integral values assigned to the methyl groups on the PDMAEMA side chains and aryl protons of the phenyldithioester end-groups respectively. The $\bar{X}_n$ for the block copolymers was determined *via* eqn (2), *vide infra*.

Size exclusion chromatography (SEC) was performed on a Shimadzu system with four phenogel columns (102, 103, 104, 106 Å pore size) in tetrahydrofuran (THF) operating at a flow rate of 1 mL min^{-1} at 40 °C using a RID-10A refractive index detector. Chromatograms were analyzed by Cirrus SEC software version 3.0. The system was calibrated with a series of narrow molecular weight distribution polystyrene standards with molecular weights ranging from 0.58–1820 kg mol^{-1}.

Transmission electron microscopy (TEM) imaging was conducted at 100 kV on a JEOL1400 TEM. To prepare TEM samples, 5.0 μL of a dilute copolymer solution (2 mg mL^{-1}) was deposited onto a copper grid (ProSciTech), stained with uranyl acetate, and dried under ambient conditions.

DLS measurements were performed using a Malvern Instrument Zetasizer Nano Series instrument equipped with a 4 mW He–Ne laser operating at 633 nm and an avalanche photodiode (APD) detector. The scattered light was detected at an angle of 173°. For sample preparation, 0.1 mL of the parent RAFTDP solution was diluted with 2.9 mL of ethanol and the solution then sonicated for 5 min prior to double filtration through 0.45 μm nylon filters.

Results and discussion

In this study, poly[2-(dimethylamino)ethyl methacrylate] (PDMAEMA) has been utilized as a RAFT macro-CTA to polymerize 2-phenylethyl methacrylate (PEMA) *via* RAFT dispersion polymerization (RAFTDP) in ethanol at 70 °C, Scheme 1. PEMA was chosen in this study as the potential core-forming block since it has never before been evaluated in RAFTDP formulations but given its structural similarity to benzyl methacrylate (BzMA), which has recently been reported to undergo facile RAFTDP in alcoholic and mixed aqueous media,[40,51] was anticipated to be a viable comonomer in such systems.

First, several RAFT homopolymerizations of DMAEMA were conducted in acetonitrile at 70 °C for 6 h to give a small family of PDMAEMA macro-CTAs of varying average degrees of polymerization ($\bar{X}_n$). After purification and isolation by precipitation into excess *n*-hexane, the chemical structure of the resulting DMAEMA homopolymers was confirmed by ^{1}H NMR spectroscopy, Fig. 1. End group analysis (accomplished by comparing

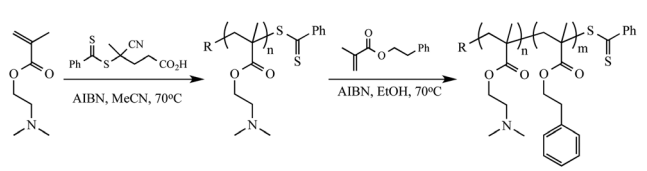

Scheme 1 RAFT synthesis of poly[2-(dimethylamino)ethyl methacrylate] (PDMAEMA) macro-CTAs and their subsequent use in the RAFT dispersion polymerization of 2-phenylethyl methacrylate in ethanol at 70 °C.

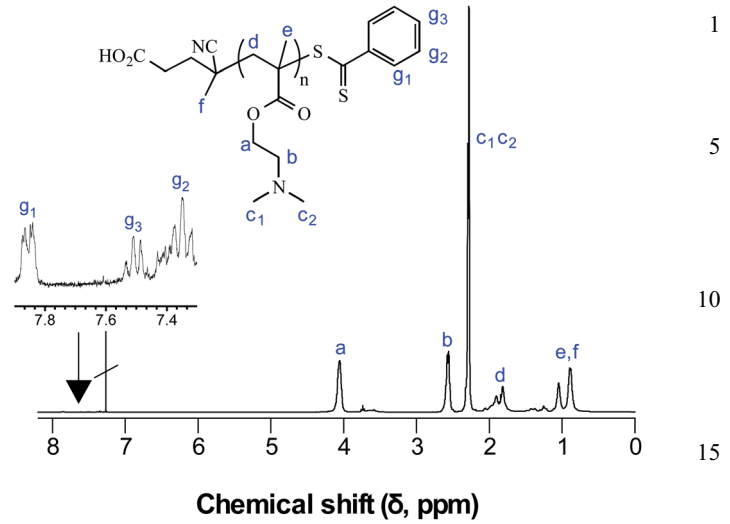

Fig. 1 ^{1}H NMR spectrum of PDMAEMA, recorded in $CDCl_3$, with peak assignments. Inset is an expanded region highlighting the presence of the phenyldithioester end group hydrogen's.

the integrals of any, or all, of the phenyl end group hydrogens labelled g_1–g_3 with any of the clear and distinct DMAEMA-associated resonances labelled a, b, or c_1 and c_2) indicated the group of PDMAEMA macro-CTAs had $\bar{X}_n$'s of 26 ($\bar{M}_{n,NMR} = 3800$, $Đ_{M,SEC} = 1.14$), 45 ($\bar{M}_{n,NMR} = 6800$, $Đ_{M,SEC} = 1.14$), 59 ($\bar{M}_{n,NMR} = 9000$, $Đ_{M,SEC} = 1.12$), and 92 ($\bar{M}_{n,NMR} = 14\,200$, $Đ_{M,SEC} = 1.16$). These were subsequently employed as the macro-CTAs in the RAFTDP of PEMA.

When evaluating the RAFTDP of a given substrate there are a number of variables that can be changed when identifying reaction conditions leading to the formation of a specific self-assembled morphology. These include the effect of $\bar{X}_n$ of the solvophobic block for a fixed $\bar{X}_n$ of stabilizing block, the effect of $\bar{X}_n$ of the stabilizing block for fixed or variable $\bar{X}_n$ of solvophobic block, the total solids concentration, the nature of the solvent (especially where a homologous series may be of interest, *i.e.* lower alcohols), and the effect of initiator concentration. For the target $DMAEMA_x$–$PEMA_y$ diblock copolymers in this study, we systematically varied and evaluated (i) the target $\bar{X}_n$ of the solvophobic PEMA block, *i.e.* the value of y, for a fixed value of x, (ii) the $\bar{X}_n$ of the solvophilic DMAEMA block, x, and (iii) the total solids content at which the RAFTDPs were conducted. We also note at this point that in preliminary experiments in alcoholic media we noticed that in some instances ionization of the DMAEMA residues had occurred giving a weak, cationic polyelectrolytic species. Since ionization of the stabilizing block can have an effect on the self-assembly process,[38,52] all the block copolymerizations discussed below were performed in the presence of NEt_3 to negate possible ionization of the DMAEMA residues.

Effect of PEMA $\bar{X}_n$ at a fixed concentration and fixed PDMAEMA $\bar{X}_n$

In the initial series of experiments the PDMAEMA macro-CTA with an $\bar{X}_n$ of 45 was employed to polymerize PEMA in

Table 1 Monomer conversion, NMR-determined molecular weight, SEC measured $\bar{M}_n$ and dispersities, intensity–average particle diameters and DLS polydispersity (μ_2/I^{-2}) and morphologies obtained for PDMAEMA$_{45}$-*b*-PPEMA$_y$ diblock copolymer nanoparticles prepared *via* RAFT dispersion polymerization of PEMA in ethanol at 70 °C with increasing [monomer]/[macro-CTA] ratio

PDMAEMA-*b*-PPEMA composition[a]	[Monomer]/[macro-CTA][a]	PEMA% conv.[b]	$\bar{M}_{n,NMR}$[c] ($\bar{M}_{n,SEC}$)	$Đ_M$[d]	Hydrodynamic diameter[e] (nm)	μ_2/I^{-2}	TEM morphology
PDMAEMA$_{45}$-*b*-PPEMA$_{46}$	50	90	16 100 (8150)	1.38	27	0.21	Spheres
PDMAEMA$_{45}$-*b*-PPEMA$_{73}$	75	97	21 200 (9150)	1.18	27	0.46	Spheres + worms
PDMAEMA$_{45}$-*b*-PPEMA$_{91}$	100	90	24 700 (17 500)	1.16	43	0.30	Spheres + worms
PDMAEMA$_{45}$-*b*-PPEMA$_{143}$	150	95	34 600 (22 100)	1.40	512	0.67	Worms + vesicles
PDMAEMA$_{45}$-*b*-PPEMA$_{186}$	200	93	42 700 (26 500)	1.36	203	0.43	Worms + vesicles
PDMAEMA$_{45}$-*b*-PPEMA$_{208}$	250	89	46 900 (28 750)	1.21	187	0.54	Vesicles
PDMAEMA$_{45}$-*b*-PPEMA$_{344}$	800	43	63 500 (36 150)	1.54	170	0.32	Vesicles

[a] Molar ratio. [b] As determined by ^{1}H NMR spectroscopy. [c] As determined by ^{1}H NMR spectroscopy and end group analysis. [d] As determined by size exclusion chromatography. [e] As determined by dynamic light scattering.

ethanol at a fixed total solids content of 29 wt%. This particular macro-CTA was chosen since its $\bar{X}_n$ is not dissimilar to that of the PDMAEMA macro-CTA employed by Jones *et al.* in their studies of the RAFTDP of BzMA in alcoholic media in which a range of self-assembled morphologies were observed.[38] Given that the primary factor controlling the self-assembled morphology of a block copolymer in a selective solvent is the ratio (relative mass or volume fraction) of the solvophilic and solvophobic building blocks[18,25,53] (often discussed in terms of the geometric packing parameter, $p = v/a_0 l_c$ where v is the volume of the hydrophobic segment, a_0 is the contact area of the head group and l_c is the length of the hydrophobic segment)[25,54–56] this series of experiments was conducted since it facilitated control of this ratio, thus giving the best chance of capturing a range of different self-assembled nanoparticle morphologies.

A series of RAFTDPs were performed with targeted final compositions ranging from the near symmetric PDMAEMA$_{45}$-*b*-PPEMA$_{50}$ to the highly asymmetric PDMAEMA$_{45}$-*b*-PPEMA$_{800}$. In all instances polymerizations started homogeneous and became increasing milky, *i.e.* heterogeneous, as conversion increased. In each case polymerizations were run for 18 h. After this time aliquots were withdrawn and the resulting block copolymers isolated by repeated precipitations into *n*-hexane followed by drying *in vacuo* at 40 °C prior to analysis. ^{1}H NMR spectroscopy was used to evaluate the final copolymer composition and absolute molecular weight and size exclusion chromatography (SEC) was employed to measure the polystyrene-equivalent $\bar{M}_n$ and $Đ_M$. The results of these measurements are summarized in Table 1 while a representative ^{1}H NMR spectrum of a DMAEMA$_{45}$-*b*-PEMA$_{208}$ copolymer is shown in Fig. 2A, and measured SEC traces of select block copolymers are shown in Fig. 2B.

^{1}H NMR analysis indicated that under the adopted conditions the block copolymerizations proceeded to high conversion of PEMA monomer (>89%) with the exception of the PDMAEMA$_{45}$-*b*-PPEMA$_{800}$ targeted species which only reached 43% conversion but still yielded a highly asymmetric block copolymer with a final composition of PDMAEMA$_{45}$-*b*-PPEMA$_{344}$. SEC analysis indicated that all the isolated AB diblock copolymers had reasonably low dispersities ($Đ_M \leq$

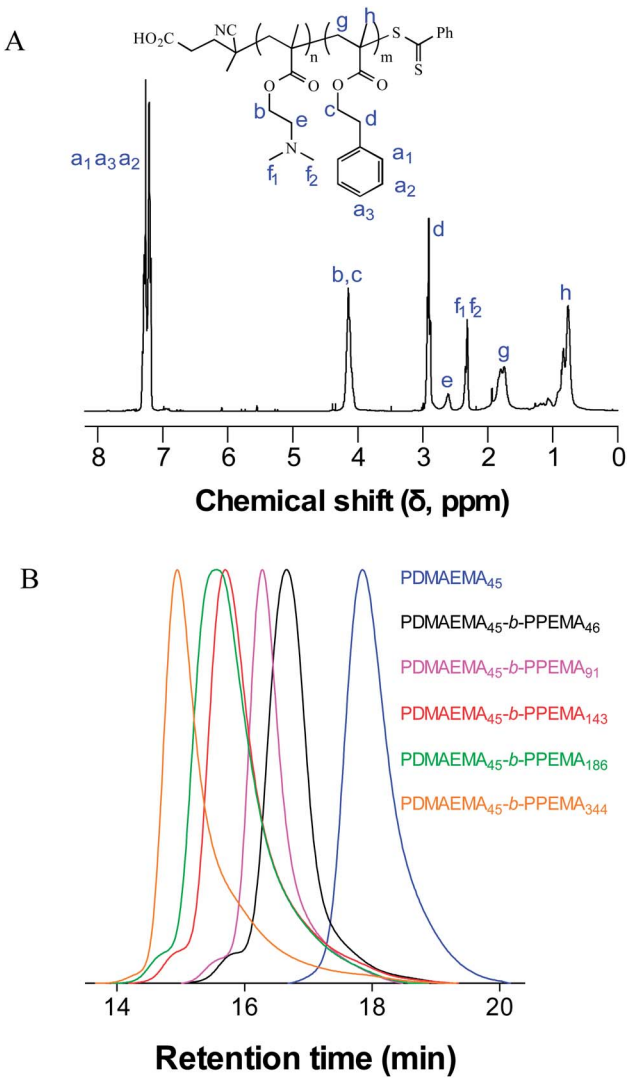

Fig. 2 ^{1}H NMR spectrum, recorded in $CDCl_3$, of the PDMAEMA$_{45}$-*b*-PPEMA$_{208}$ block copolymer (A), and representative size exclusion chromatograms of the resulting PDMAEMA$_x$-*b*-PPEMA$_y$ copolymers obtained by RAFTDP (B).

1.40), again with the exception of the final sample, which had a slightly larger $Đ_M$ of 1.54. While the molecular weight distributions of the block copolymers are relatively narrow, there is clear evidence in each case of a higher molecular weight impurity whose origins are due to polymer–polymer radical termination reactions.[57,58] While this is not uncommon in RAFT (co)polymerizations, including RAFTDP systems,[37,51,59,60] it can become particularly prevalent in polymerizations taken to high conversions such as those described here.

The absolute molecular weight, $\bar{M}_{n,NMR}$ and $\bar{X}_n$ of the PDMAEMA$_{45}$-*b*-PPEMA$_y$ copolymers was calculated based on the $\bar{X}_n$ of the PDMAEMA macro-CTA and the integration ratio of the signals at δ = 7.10–7.50 ppm ($I_{7.10-7.50ppm}$, a_1, a_2, a_3, aryl protons of PPEMA) to those at 2.30 ppm ($I_{2.30ppm}$, f_1, f_2, methyl protons of PDMAEMA), as shown in Fig. 2A and eqn (2).

$$\overline{X}_n(\text{PPEMA}) = \frac{6 \times I\ (7.10\ -\ 7.50\ \text{ppm})}{5 \times I\ (2.30\ \text{ppm})}\overline{X}_n(\text{PDMAEMA}) \quad (2)$$

In addition to the above characterization, the final self-assembled nanoparticles were imaged directly *via* transmission electron microscopy (TEM). For the given fixed solids content and $\bar{X}_n$ of the DMAEMA block a clear morphological transition from spheres to worms to vesicles was observed with increasing [monomer]/[PDMAEMA$_{45}$], *i.e.* with increasing values of *y* in PDMAEMA$_{45}$-*b*-PPEMA$_y$, Fig. 3.

In the case of the near symmetric species, PDMAEMA$_{45}$-*b*-PPEMA$_{46}$ (Fig. 3A), the final morphology observed was spherical in nature with a narrow size distribution and a TEM-estimated average diameter of *ca.* 20.0 nm. This size agrees very well with the hydrodynamic diameter measured by dynamic light scattering (DLS) of 27.0 nm (μ_2/Γ^2 = 0.21). The discrepancy between TEM and DLS is common and is a direct reflection of the sizes being measured in solution (DLS) *vs.* the solid state (TEM). The formation of spherical particles at this essentially symmetric composition falls within the general broad compositional range where spherical aggregates may be expected. Increasing the $\bar{X}_n$ of the PEMA block to 73 (PDMAEMA$_{45}$-*b*-PEMA$_{73}$, Fig. 3B) results in a mixed morphology with spheres and worms being present in roughly equal amounts. While predictive methods like the packing parameter suggest distinct morphological transitions at certain values of *p* it is worth remembering that the shape factor concept was devised by Israelachvili, Mitchell and Ninham[61] to describe the behaviour of conventional small molecule amphiphiles whereas we are dealing with 'high' molecular weight copolymers and their associated molecular weight (dispersity) and compositional distributions superimposed on one another. As such it is not surprising that mixed phases are observed at or near certain key compositions. As expected, the average, TEM-determined, diameter of the worms (averaged from measurements on ten different species) is *ca.* 21.0 nm, essentially identical to the measured diameter of the spheres. Increasing the $\bar{X}_n$ of the PEMA block further to give PDMAEMA$_{45}$-*b*-PPEMA$_{91}$ (Fig. 3C) also results in a mixed morphology of spheres and worms, with the latter now being the predominant morphology and the diameters of both the aggregate species appear to be significantly larger than in the samples with lower PEMA contents. This is not unexpected since increasing the molecular weight of a copolymer in a given morphological range will result in aggregates of a larger size.[25] In the case of PDMAEMA$_{45}$-*b*-PPEMA$_{143}$ (Fig. 3D) another mixed morphology phase of predominantly worms but with evidence of vesicles is seen. In this case the average TEM-measured diameter of the worms is *ca.* 30.0 nm (note: since DLS is based on the Stokes–Einstein equation which assumes the presence of solid spheres, the hydrodynamic diameters reported for mixed phases with non-spherical species represent 'sphere-equivalent' sizes and clearly should be treated with caution). PDMAEMA$_{45}$-*b*-PPEMA$_{186}$ (Fig. 3E) forms aggregates in which vesicles (of a fairly uniform size) represent the major morphology while the two most asymmetric block copolymers, PDMAEMA$_{45}$-*b*-PPEMA$_{208}$ and PDMAEMA$_{45}$-*b*-PPEMA$_{344}$ form only vesicles. Unlike the mixed phases the TEM-estimated size of these vesicles (*ca.* 150–180 nm) is in reasonable agreement with those measured by DLS of *ca.* 190 nm. These observed morphological transitions as a function of increasing $\bar{X}_n$ of the PEMA block are broadly consistent with the observations made by Jones *et al.* in their RAFTDP studies of PDMAEMA-*b*-PBzMA copolymers.[38]

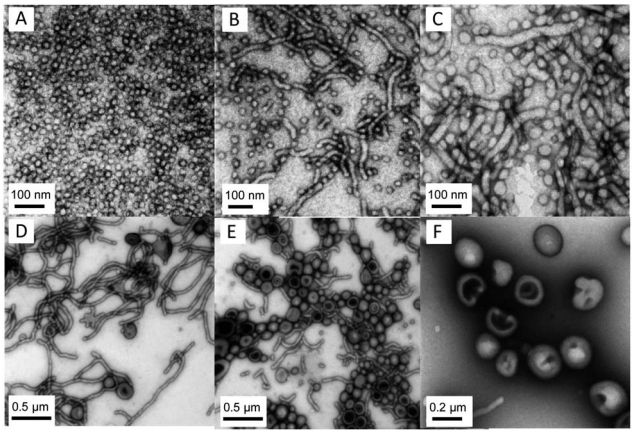

Fig. 3 Representative TEM images obtained for PDMAEMA$_{45}$-*b*-PPEMA$_y$ diblock copolymer nanoparticles synthesized at a total solids concentration of 29 wt% using RAFT dispersion polymerization in ethanol at 70 °C with a PDMAEMA$_{45}$ macro-CTA, AIBN initiator and using targeted [monomer]/[macro-CTA] molar ratios of (A) 50, (B) 75, (C) 100, (D) 150, (E) 200 and (F) 250.

Effect of total solids content for a fixed target composition

The effect of copolymer concentration on the final observed morphology can also be an important parameter when targeting a specific self-assembled state since concentration can affect the aggregation number (N_{agg} – the number of block copolymer chains in a self-assembled structure) which in turn can affect the molecular curvature and hence the particle morphology.[25] In the next series of experiments we evaluated the effect of total solids content on the ethanolic RAFTDP of PEMA with the PDMAEMA$_{45}$ macro-CTA for a targeted PEMA $\bar{X}_n$ of 100 at

Table 2 NMR-determined monomer conversion and molecular weights, SEC-measured dispersities, intensity–average particle diameters and morphologies obtained for targeted $PDMAEMA_{45}$-*b*-$PPEMA_{100}$ diblock copolymer particles prepared *via* RAFT dispersion polymerization of 2-phenylethyl methacrylate in ethanol at 70 °C at various solids content

		NMR		SEC	DLS		TEM
PDMAEMA-*b*-PPEMA composition[a]	Solids content (w/w)	PEMA% conv.[a]	$\bar{M}_{n,NMR}$[b] ($\bar{M}_{n,SEC}$)	$Đ_M$[c]	Diameter[d] (nm)	μ_2/I^2	Morphology
$PDMAEMA_{45}$-*b*-$PPEMA_{95}$	10%	95	25 700 (8800)	1.12	44	0.12	Spheres
$PDMAEMA_{45}$-*b*-$PPEMA_{95}$	20%	95	24 800 (9050)	1.21	49	0.21	Worms
$PDMAEMA_{45}$-*b*-$PPEMA_{98}$	29%	98	25 400 (9700)	1.20	61	0.19	Worms
$PDMAEMA_{45}$-*b*-$PPEMA_{99}$	40%	99	25 600 (10 000)	1.22	52	0.23	Worms

[a] As determined by ^{1}H NMR spectroscopy. [b] As determined by ^{1}H NMR spectroscopy and end group analysis. [c] As determined by size exclusion chromatography. [d] As determined by dynamic light scattering.

concentrations ranging from 10–40 wt% total solids. The results are summarized in Table 2.

In all instances high conversions of PEMA were obtained (≥95%) and all final block copolymers had comparable molecular weights as judged by ^{1}H NMR spectroscopy, as expected. Similarly, SEC indicated that all samples had comparable dispersities with measured values between 1.12 and 1.22.

While NMR and SEC indicated that each of the parent DMAEMA–PEMA block copolymers were structurally virtually identical, TEM analysis, Fig. 4, indicated that the final self-assembled nanoparticles did possess different morphologies. In the case of the RAFTDP conducted at 10 wt% solids, TEM revealed particles with a spherical morphology and narrow size distribution with an average size of *ca.* 32.0 nm. This is in reasonable agreement with the DLS-measured hydrodynamic diameter of 44.0 nm ($\mu_2/I^2 = 0.12$). For all remaining concentrations evaluated the primary observed morphology was worms with essentially identical average core diameters as would be anticipated for polymers of an 'identical' molecular weight and composition. While these experiments demonstrate an effect of concentration of the final self assembled morphology, it is not especially pronounced at the block copolymer composition targeted.

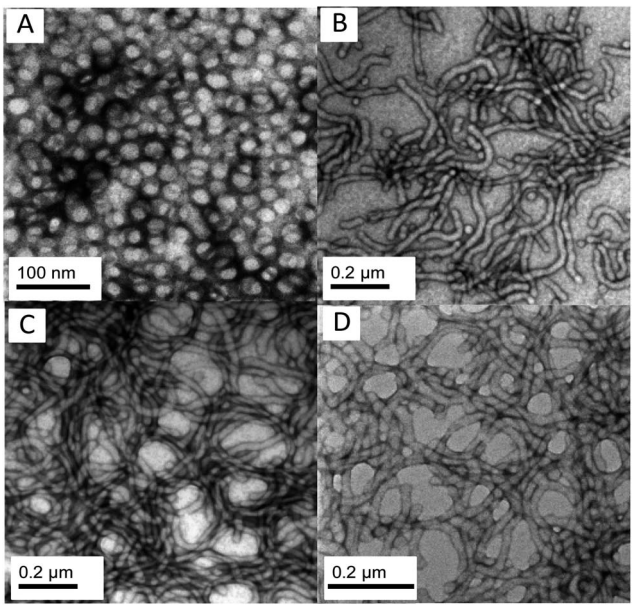

Fig. 4 Representative TEM images obtained for $PDMAEMA_{45}$-*b*-$PPEMA_{100}$ diblock copolymer nanoparticles synthesized at a total solids concentration of (A) 10%, (B) 20%, (C) 29% and (D) 40% using RAFT dispersion polymerization in ethanol at 70 °C with a $PDMAEMA_{45}$ macro-CTA, AIBN initiator and using a [monomer]/[macro-CTA] molar ratio of 100.

Effect of $\bar{X}_n$ of the PDMAEMA stabilizing block

Next, the effect of the $\bar{X}_n$ of the PDMAEMA stabilizing block in a series of RAFTDPs conducted at 29 wt% for a targeted, *fixed*, $\bar{X}_n$ of the PEMA block of 100 was examined. These experiments were performed to demonstrate that it is also possible to control particle morphology by varying the $\bar{X}_n$ of the solvophilic block for a fixed solvophobic block length. The results of these experiments are summarized in Table 3. In all instances very high to near quantitative conversions were obtained as judged by ^{1}H NMR spectroscopy and dispersities of the AB diblock copolymers spanned the range 1.16–1.66.

TEM revealed the expected morphology change with increasing $\bar{X}_n$ of the PDMAEMA macro-CTAs. For the lowest $\bar{X}_n$ macro-CTA a mixed morphology of vesicles and worms was observed (Fig. 5A). Increasing the $\bar{X}_n$ of the PDMAEMA macro-CTA to 45 (increasing the solvophilic-to-solvophobic ratio) gave a pure worm nanoparticle phase (5B) while in the case of the two highest molecular weight PDMAEMA macro-CTAs pure phases of spherical nanoparticles were observed whose 26 nm) diameters (22 and 26 agreed reasonably well with those determined by DLS, Table 3 and Fig. 5C and D. These 'reverse' morphological transitions from higher ordered structures (vesicles) to more simple self-assembled species (spheres) for an increasing $\bar{X}_n$ of PDMAEMA is a direct result of the increasing solvophilic/solvophobic ratio, *i.e.* moving from highly asymmetric to near symmetric block copolymers.

However, we note that while these results clearly demonstrate that it is possible to control, or target, specific self-assembled nanoparticle morphologies in a RAFTDP formulation by varying the $\bar{X}_n$ of the solvophilic *or* solvophobic block, as well as controlling total solids content, Jones and

Table 3 Monomer conversion, the NMR-determined number average molecular weight, dispersities, intensity-average particle diameters and polydispersities as determined by DLS, and TEM-observed morphologies obtained for PDMAEMA$_x$-*b*-PPEMA$_{100}$ prepared *via* RAFTDP of 2-phenylethyl methacrylate in ethanol at 70 °C at a fixed solids concentration of 29 wt%

	NMR		SEC	DLS		TEM
PDMAEMA-*b*-PPEMA composition[a]	PEMA% conv.[a]	$\bar{M}_{n,NMR}$[b] ($\bar{M}_{n,SEC}$)	$Đ_M$[c]	Diameter[d] (nm)	μ_2/I^2	Morphology
PDMAEMA$_{26}$-*b*-PPEMA$_{96}$	96	13 400 (7100)	1.66	43	0.30	Vesicles + worms
PDMAEMA$_{45}$-*b*-PPEMA$_{90}$	90	25 000 (9200)	1.16	227	0.31	Worms
PDMAEMA$_{59}$-*b*-PPEMA$_{97}$	97	27 800 (17 500)	1.20	23	0.12	Spheres
PDMAEMA$_{92}$-*b*-PPEMA$_{97}$	97	33 200 (22 700)	1.50	45	0.13	Spheres

[a] As determined by ^{1}H NMR spectroscopy. [b] As determined by ^{1}H NMR spectroscopy and end group analysis. [c] As determined by size exclusion chromatography. [d] As determined by dynamic light scattering.

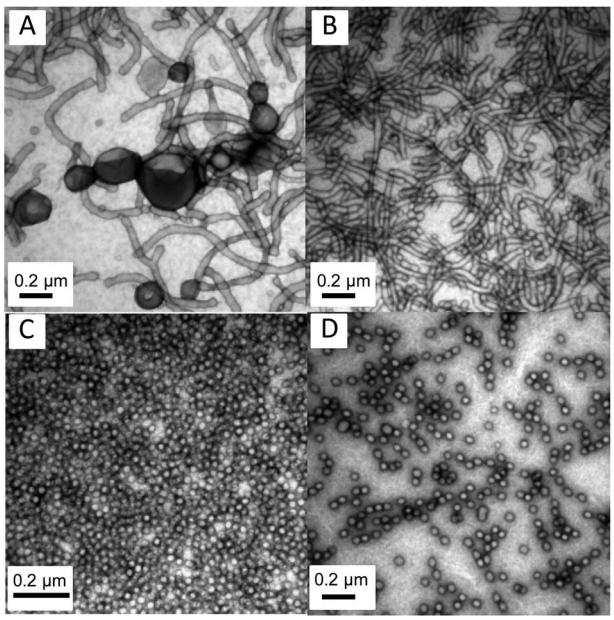

Fig. 5 Representative TEM images obtained for PDMAEMA$_x$-*b*-PPEMA$_{100}$ diblock copolymer nanoparticles synthesized at a total solids concentration of 29 wt% by RAFTDP in ethanol at 70 °C with (A) PDMAEMA$_{26}$, (B) PDMAEMA$_{45}$, (C) PDMAEMA$_{59}$, (D) DMAEMA$_{92}$ macro-CTAs and AIBN as the source of primary radicals and employing a [monomer]/[macro-CTA] molar ratio of 100.

co-workers evaluated the RAFTDP of BzMA with a PDMAEMA macro-CTA with $\bar{X}_n = 74$ at a concentration of 10 wt% with target block lengths of the BzMA block ranging from 100–1000. In all instances the authors reported the formation of *only* spheres that increased in size with increasing $\bar{X}_n$ of the BzMA block. The formation of a single self-assembled morphology was attributed to the higher copolymer curvature associated with the higher $\bar{X}_n$ of the solvophilic PDMAEMA block.[38] While the $\bar{X}_n$ of the solvophilic block can be used to control particle morphology, as demonstrated here, this clearly suggests that straightforward access to a range of different particle morphologies may best be suited to the use of a solvophilic stabilizing block of relatively low $\bar{X}_n$ while controlling the $\bar{X}_n$ of the solvophobic block.

Conversion of nanoparticles to polysulfopropylbetaine derivatives

One pertinent feature of polymeric nanoparticles with tertiary amine residues in the coronal layer is that as reactive species they can be modified to quaternary ammonium species before or after polymerization *via* simple alkylation or, more simply, by adjusting the pH of an aqueous dispersion.[38,52] Besides quaternary ammonium species, the tertiary amine functional groups in PDMAEMA (co)polymers can also be readily converted to the corresponding poly(sulfopropylbetaine)s by reaction with 1,3-propanesultone.[62–64]

To highlight the ease of such functional group conversions, the self-assembled PDMAEMA$_{45}$-*b*-PPEMA$_{98}$ block copolymer was reacted with a 10 mol% excess (based on DMAEMA residues) of 1,3-propanesultone in ethanol at RT, Scheme 2.

As expected, the resulting sulfopropylbetaine derivative (PDMAEMASB$_{45}$-*b*-PPEMA$_{98}$, SB = sulfobetaine) formed a macroscopic white precipitate consistent with the limited solubility features of such zwitterionic derivatives. After purification and drying the extent of betainization was determined by ^{1}H NMR spectroscopy using deuterated trifluoroacetic acid (d_1-TFA) as the solvent, a good solvent for both the DMAEMASB and PEMA blocks, Fig. 6.

The key indicator for successful, and quantitative, reaction is the shift of the signal associated with the dimethylamino hydrogen's from *ca.* $\delta = 2.4$ ppm in the parent block copolymer to *ca.* 3.4 ppm in the sulfopropylbetaine derivative. In addition, we observe the appearance of new signals (e, i, g Fig. 6B)

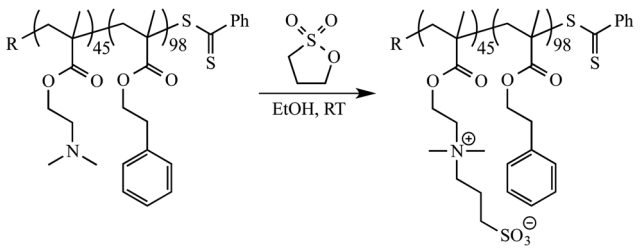

Scheme 2 Betainization of the DMAEMA resides in PDMAEMA$_{45}$-*b*-PPEMA$_{98}$ from the reaction of the tertiary amine residues with 1,3-propanesultone.

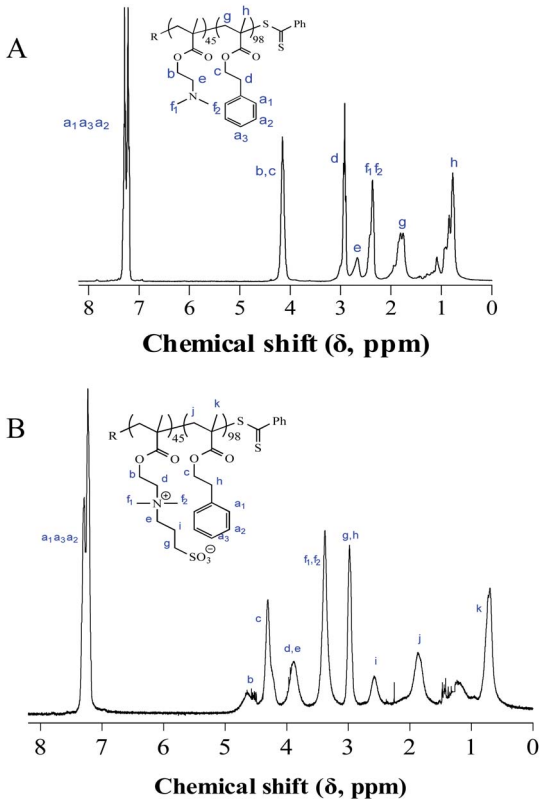

Fig. 6 ^{1}H NMR spectra of the PDMAEMA$_{45}$-*b*-PPEMA$_{98}$ precursor block copolymer recorded in $CDCl_3$ (A) and the corresponding sulfopropylbetaine derivative, PDMAEMASB$_{45}$-*b*-PPEMA$_{98}$, recorded in d_1-TFA (B).

associated with the methylene hydrogen's situated between the quaternary ammonium group and the sulfonate species. These observations are consistent with previous reports on the modification of DMAEMA residues in homo and block copolymers with 1,3-propanesultone.[62,65]

Having confirmed successful modification of the PDMAEMA$_{45}$-*b*-PPEMA$_{98}$ parent copolymer to its sulfopropylbetaine derivative we next examined the morphology after redispersing the nanoparticles in water. The TEM images for the parent and sulfopropylbetaine derivative imaged from solutions of the same concentration are shown in Fig. 7A and B. Fig. 7A is the same species as shown in Fig. 4C and is included again here for ease of comparison. As noted above, at 29 wt% in ethanol the PDMAEMA$_{45}$-*b*-PPEMA$_{98}$ block copolymer formed a single phase consisting of worms. In contrast, the sulfopropylbetaine species appears to form mixed morphologies with both spheres and worms being observed, with the latter being the major component. Since both species have identical $\bar{X}_n$'s and compositions, were analyzed at identical concentrations, and have v/l_c values that we assume are identical, this change in morphology must be due to either a change in N_{agg} upon betainization, the nature of the solvent (ethanol *vs.* water), or a change in a_o. With respect to the nature of the solvent, Jones *et al.*[38] noted that when PDMAEMA$_{31}$-*b*-PBzMA$_y$ (y = 40 (spheres), 80 (worms), or 120 (vesicles)) were dispersed in ethanol, water at pH 3 (DMAEMA residues expected to be protonated) and water at pH 10 (DMAEMA residues expected to be essentially deprotonated) that the original ethanol-based morphologies were unchanged, *i.e.* the cationic species behaved in a manner essentially identical to that of the neutral species and the transfer/re-dispersal of the nanoparticles from alcoholic to aqueous media had little-to-no effect on the solution morphology.

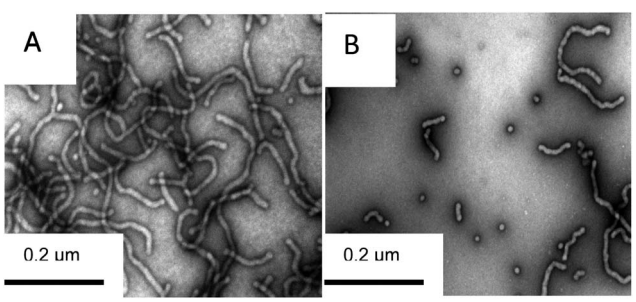

Fig. 7 Representative TEM images of the PDMAEMA$_{45}$-*b*-PPEMA$_{98}$ parent worm nanoparticles (A) and the same polymer, at the same concentration after conversion of the DMAEMA residues to the sulfopropylbetaine analogues (B).

For our system, N_{agg} is unknown, but arguably unlikely to change readily after polymerization since the T_g of PPEMA is reported to be *ca.* 42 °C[49,66] and as such the aggregates can be considered essentially kinetically frozen at ambient temperature. As noted above, Jones reported that the nature of the continuous phase (ethanol *vs.* aqueous media) had little, or no, effect on the solution morphology for structurally similar, albeit cationic, nanoparticles. As such, we assume the difference in morphology is due to features associated with the betaine coronal block. While such zwitterions are electrically neutral there are net positive attractive forces between such species commonly resulting in highly compact structures for such species.[67] This may result in increased curvature and account for the possible presence of some nanoparticles with a spherical morphology. However, the exact reason for this apparent morphological transition is unclear and we are currently investigating this in more detail.

Conclusions

Herein we have described the first examples of RAFT dispersion polymerization (RAFTDP) of 2-phenylethyl methacrylate (PEMA). RAFTDPs were performed in ethanol employing poly[2-(dimethylamino)ethyl methacrylate]s (PDMAEMAs) as macro chain transfer agents (macro-CTA). We demonstrated that control of the resulting block copolymer composition and overall concentration of the polymerizations had a pronounced effect on the resulting nanoparticle morphology with spheres, cylinders and vesicles (and various mixed phases) all being observed under specific reaction conditions. Of the various factors, the effect of copolymer composition for a relatively low molecular weight PDMAEMA macro-CTA was the most pronounced while total solids had a less pronounced effect. Additionally, it was shown that the morphology could also be controlled in the 'reverse' fashion by varying the average block length of the solvophilic DMAEMA block for a constant $\bar{X}_n$ of

PEMA. Finally, we reported the first examples of sulfopropylbetaine nanoparticles prepared using the RAFTDP process as the synthetic tool. Interestingly, conversion of the parent PDMAEMA-*b*-PPEMA copolymer to the betaine analogue was accompanied with a morphological transition from a pure worm phase to a mixed sphere/worm phase.

Acknowledgements

ABL thanks the Australian Research Council for funding *via* a Future Fellowship (FT110100046) and Discovery Grant (DP110104391).

Notes and references

1 G. Moad, E. Rizzardo and S. H. Thang, *Aust. J. Chem.*, 2005, **58**, 379–410.
2 G. Moad, E. Rizzardo and S. H. Thang, *Aust. J. Chem.*, 2006, **59**, 669–692.
3 G. Moad, E. Rizzardo and S. H. Thang, *Aust. J. Chem.*, 2012, **65**, 985–1076.
4 G. Moad, J. Chiefari, Y. K. Chong, J. Krstina, R. T. A. Mayadunne, A. Postma, E. Rizzardo and S. H. Thang, *Polym. Int.*, 2000, **49**, 993–1001.
5 G. Moad, Y. K. Chong, A. Postma, E. Rizzardo and S. H. Thang, *Polymer*, 2005, **46**, 8458–8468.
6 A. B. Lowe and C. L. McCormick, *Prog. Polym. Sci.*, 2007, **32**, 283–351.
7 C. Boyer, V. Bulmus, T. P. Davis, V. Ladmiral, J. Liu and S. Perrier, *Chem. Rev.*, 2009, **109**, 5402–5436.
8 M. Ahmed and R. Narain, *Prog. Polym. Sci.*, 2013, **38**, 767–790.
9 A. Gregory and M. H. Stenzel, *Prog. Polym. Sci.*, 2012, **37**, 38–105.
10 A. E. Smith, X. Xu and C. L. McCormick, *Prog. Polym. Sci.*, 2010, **35**, 45–93.
11 G. Riess, *Prog. Polym. Sci.*, 2003, **28**, 1107–1170.
12 J. Rodriguezhernandez, F. Checot, Y. Gnanou and S. Lecommandoux, *Prog. Polym. Sci.*, 2005, **30**, 691–724.
13 Y. Yu and A. Eisenberg, *J. Am. Chem. Soc.*, 1997, **119**, 8383–8384.
14 T. Gadt, N. S. Ieong, G. Cambridge, M. A. Winnik and I. Manners, *Nat. Mater.*, 2009, **8**, 144–150.
15 J. Xu, Y. Zhu, J. Zhu and W. Jiang, *Nanoscale*, 2013, **5**, 6344–6349.
16 D. E. Discher and A. Eisenberg, *Science*, 2002, **297**, 967–973.
17 M. Antonietti and S. Förster, *Adv. Mater.*, 2003, **15**, 1323–1333.
18 D. E. Discher and F. Ahmed, *Annu. Rev. Biomed. Eng.*, 2006, **8**, 323–341.
19 L. Alexander, K. Dhaliwal, J. Simpson and M. Bradley, *Chem. Commun.*, 2008, 3507–3509.
20 J. R. Howse, R. A. L. Jones, G. Battaglia, R. E. Ducker, G. J. Leggett and A. J. Ryan, *Nat. Mater.*, 2009, **8**, 507–511.
21 V. Ladmiral, M. Semsarilar, I. Canton and S. P. Armes, *J. Am. Chem. Soc.*, 2013, **135**, 13574–13581.
22 P. P. Ghoroghchian, P. R. Frail, K. Susumu, T.-H. Park, S. P. Wu, H. T. Uyeda, D. A. Hammer and M. J. Therien, *J. Am. Chem. Soc.*, 2005, **127**, 15388–15390.
23 J. Y. Cheng, A. M. Mayes and C. A. Ross, *Nat. Mater.*, 2004, **3**, 823–828.
24 A. Kishimura, A. Koide, K. Osada, Y. Yamasaki and K. Kataoka, *Angew. Chem., Int. Ed.*, 2007, **46**, 6085–6088.
25 Y. Mai and A. Eisenberg, *Chem. Soc. Rev.*, 2012, **41**, 5969–5985.
26 E. B. Zhulina, M. Adam, I. LaRue, S. S. Sheiko and M. Rubinstein, *Macromolecules*, 2005, **38**, 5330–5351.
27 D. Roy, J. N. Cambre and B. S. Sumerlin, *Prog. Polym. Sci.*, 2010, **35**, 278–301.
28 J.-T. Sun, C.-Y. Hong and C.-Y. Pan, *Polym. Chem.*, 2013, **4**, 873–881.
29 B. Charleux, G. Delaittre, J. Rieger and F. D'Agosto, *Macromolecules*, 2012, **45**, 6753–6765.
30 Z. An, Q. Shi, W. Tang, C.-K. Tsung, C. J. Hawker and G. D. Stucky, *J. Am. Chem. Soc.*, 2007, **129**, 14493–14499.
31 Y. Li and S. P. Armes, *Angew. Chem., Int. Ed.*, 2010, **49**, 4042–4046.
32 S. Sugihara, A. Blanazs, S. P. Armes, A. J. Ryan and A. L. Lewis, *J. Am. Chem. Soc.*, 2011, **133**, 15707–15713.
33 A. Blanazs, A. J. Ryan and S. P. Armes, *Macromolecules*, 2012, **45**, 5099–5107.
34 P. Chambon, A. Blanazs, G. Battaglia and S. P. Armes, *Macromolecules*, 2012, **45**, 5081–5090.
35 J. Rosselgong, A. Blanazs, P. Chambon, M. Williams, M. Semsarilar, J. Madsen, G. Battaglia and S. P. Armes, *ACS Macro Lett.*, 2012, **1**, 1041–1045.
36 M. Semsarilar, V. Ladmiral, A. Blanazs and S. P. Armes, *Langmuir*, 2012, **28**, 914–922.
37 L. P. D. Ratcliffe, A. J. Ryan and S. P. Armes, *Macromolecules*, 2013, **46**, 769–777.
38 E. R. Jones, M. Semsarilar, A. Blanazs and S. P. Armes, *Macromolecules*, 2012, **45**, 5091–5098.
39 M. Semsarilar, E. R. Jones, A. Blanazs and S. P. Armes, *Adv. Mater.*, 2012, **24**, 3378–3382.
40 D. Zehm, L. P. D. Ratcliffe and S. P. Armes, *Macromolecules*, 2013, **46**, 128–139.
41 J. Rieger, C. Grazon, B. Charleux, D. Alaimo and C. Jérôme, *J. Polym. Sci., Part A: Polym. Chem.*, 2009, **47**, 2373–2390.
42 L. Houillot, C. Bui, C. Farcet, C. Moire, J. A. Raust, H. Pasch, M. Save and B. Charleux, *ACS Appl. Mater. Interfaces*, 2010, **2**, 434–442.
43 W.-D. He, X.-L. Sun, W.-M. Wan and C.-Y. Pan, *Macromolecules*, 2011, **44**, 3358–3365.
44 W. M. Wan, X. L. Sun and C. Y. Pan, *Macromol. Rapid Commun.*, 2010, **31**, 399–404.
45 W.-M. Wan and C.-Y. Pan, *Polym. Chem.*, 2010, **1**, 1475–1484.
46 C.-Q. Huang and C.-Y. Pan, *Polymer*, 2010, **51**, 5115–5121.
47 M. Zong, K. J. Thurecht and S. M. Howdle, *Chem. Commun.*, 2008, 5942–5944.
48 J. Jennings, M. Beija, J. T. Kennon, H. Willcock, R. K. O'Reilly, S. Rimmer and S. M. Howdle, *Macromolecules*, 2013, **46**, 6843–6851.
49 H. Lee, G. Tae and Y. H. Kim, *Macromol. Res.*, 2008, **16**, 614–619.

50 S. H. Thang, Y. K. Chong, R. T. A. Mayadunne, G. Moad and E. Rizzardo, *Tetrahedron Lett.*, 1999, **40**, 2435–2438.
51 X. Zhang, J. Rieger and B. Charleux, *Polym. Chem.*, 2012, **3**, 1502–1509.
52 M. Semsarilar, V. Ladmiral, A. Blanazs and S. P. Armes, *Langmuir*, 2013, **29**, 7416–7424.
53 C. Tanford, *Science*, 1978, **200**, 1012–1018.
54 G. H. Sagar, M. A. Arunagirinathan and J. R. Bellare, *Indian J. Exp. Biol.*, 2007, **45**, 133–159.
55 K. Kita-Tokarczyk, J. Grumelard, T. Haefele and W. Meier, *Polymer*, 2005, **46**, 3540–3563.
56 R. Nagarajan, *Langmuir*, 2002, **18**, 31–38.
57 A. R. Wang and S. Zhu, *Macromol. Theory Simul.*, 2003, **12**, 196–208.
58 B. Canniccioni, S. Monge, G. David and J.-J. Robin, *Polym. Chem.*, 2013, **4**, 3676–3685.
59 L. A. Fielding, M. J. Derry, V. Ladmiral, J. Rosselgong, A. M. Rodrigues, L. P. D. Ratcliffe, S. Sugihara and S. P. Armes, *Chem. Sci.*, 2013, **4**, 2081–2087.
60 X. Zhang, S. Boissé, C. Bui, P.-A. Albouy, A. Brûlet, M.-H. Li, J. Rieger and B. Charleux, *Soft Matter*, 2012, **8**, 1130–1141.
61 J. N. Israelachvili, D. J. Mitchell and B. W. Ninham, *J. Chem. Soc., Faraday Trans. 2*, 1976, **72**, 1525–1568.
62 A. B. Lowe, N. C. Billingham and S. P. Armes, *Chem. Commun.*, 1996, 1555–1556.
63 Z. Tuzar, H. Pospisil, J. Plestil, A. B. Lowe, F. L. Baines, N. C. Billingham and S. P. Armes, *Macromolecules*, 1997, **30**, 2509–2512.
64 A. B. Lowe, N. C. Billingham and S. P. Armes, *Macromolecules*, 1999, **32**, 2141–2148.
65 V. Bütün, C. E. Bennett, M. Vamvakaki, A. B. Lowe, N. C. Billingham and S. P. Armes, *J. Mater. Chem.*, 1997, **7**, 1693–1695.
66 G. Sakellariou, A. Siakali-Kioulafa and N. Hadjichristidis, *Int. J. Polym. Anal. Charact.*, 2003, **8**, 269–277.
67 R. Knoesel, M. Ehrmann and J. C. Galin, *Polymer*, 1993, **34**, 1925–1932.